RSC Advances

PAPER

View Article Online
View Journal | View Issue

Cite this: *RSC Adv.*, 2017, **7**, 35460

Neoansamycins from *Streptomyces* sp. LZ35†

Mengyujie Liu,[a] Chunhua Lu,[a] Ruocong Tang,[b] Shanren Li,[a] Haoxin Wang[b] and Yuemao Shen *[ab]

Received 6th June 2017
Accepted 7th July 2017

DOI: 10.1039/c7ra06339c

rsc.li/rsc-advances

Previously, activation of the cryptic *nam* gene cluster led to three new naphthalenic ansamycins with unprecedented *n*-pentyl and *n*-butyl side chains from the mutant *Streptomyces* sp. SR201*nam1*OE strain. In this study, we further characterized the products of the mutant strain and six new neoansamycin congeners, namely neoansamycins D–I (**1–6**), were elucidated. Among them, compounds **1–3** feature the conserved skeleton of neoansamycins B and C but with *n*-hexyl side chains, and **4–6** are modified neoansamycins with *n*-pentyl side chains, illustrating the biosynthetic plasticity and diverse post-PKS modifications of neoansamycins.

Introduction

Ansamycins are a family of macrolactam antibiotics with remarkable potential for druggability, including the RNA polymerase inhibitor rifamycin,[1] the Hsp90 inhibitor geldanamycin,[2] and the potent microtubule inhibitors maytansinoids.[3] Over the past ten years, we have focused on discovering ansamycin-producing strains, and obtained twenty-six 3-amino-5-hydroxyl benzoic acid (AHBA) synthase gene-positive strains from plant-associated and marine-derived actinomycetes through PCR screening of AHBA synthase genes.[4] From these AHBA synthase gene-positive strains, we isolated dozens of ansamycins, including hygrocins,[5–7] divergolides,[8,9] juanlimycins,[10] ansatrienes,[11,12] and streptovaricin derivatives ansavaricins A–I.[13,14]

Recently, *Streptomyces* sp. LZ35 was activated to produce novel naphthalenic ansamycins (neoansamycins A–C) by constitutive overexpression of a LuxR family transcriptional regulatory gene,[15] and further ten new benzenic ansamycins (5,10-*seco*-neoansamycins A–J) were obtained by disrupting the *nam7* gene in the SR201*nam1*OE strain.[16] The intriguing structure diversity of the neoansamycins A–C and 5,10-*seco*-neoansamycins A–J encouraged us to search for more new congeners of neoansamycins. In this study, six new analogues of neoansamycins, namely neoansamycins D–I (**1–6**), were isolated from the fermentation products of the strain *S.* sp. SR201*nam1*OE. Their structures were elucidated on the basis of 1D-, 2D-NMR, HRESIMS analysis and X-ray single crystal diffraction. Further, the cytotoxicity and antibacterial activities of compounds **1–6** were also evaluated in this study.

Results and discussion

The strain *S.* sp. SR201*nam1*OE was cultured on ISP3 agar media for 14 days at 28 °C. The 100 L fermented agar was diced and extracted three times with EtOAc/MeOH (80 : 20, v/v) at room temperature. The crude extract was partitioned between ddH_2O and EtOAc. The EtOAc extract was further partitioned between petroleum ether (PE) and 95% aqueous MeOH. The MeOH extract (40 g) was subjected to column chromatography over Sephadex LH-20, reversed-phase (RP) C_{18} silica gel and finally semi-preparative HPLC to yield compounds **1–6** (Fig. 1).

The molecular formula of neoansamycin D (**1**) was assigned as $C_{31}H_{39}NO_6$ on the basis of high resolution ESIMS data (*m*/*z* 522.2848 for $[M + H]^+$) (ESI Fig. S13†). Interpretation of the NMR data (Tables 1 and 2) revealed that **1** had similar structure as that of neoansamycin B,[15] except for the substitute of a hexyl at C-20 instead of an amyl side chain, and which was further confirmed by the ^1H–^1H COSY and HMBC correlations (ESI Table S1 and Fig. S1†). The NOESY correlations (ESI Table S1†) from H-19 to H-18a and H-20a revealed the relative configurations of **1**. Finally, the absolute configurations of neoansamycin D were fully confirmed by the X-ray diffraction analysis (CCDC 1481243†) (Fig. 2).

The high-resolution of neoansamycin E (**2**) gave a quasi-molecular ion at *m*/*z* 540.2952 $[M + H]^+$ (ESI Fig. B19†) consistent with the molecular formula $C_{31}H_{41}NO_7$. After careful comparison the NMR data of **1** and **2**, we found compound **2** is as an analogue of **1**. The chemical shifts of C-11 (δ_C 150.3 s) and C-12 (δ_C 118.7 s) in **1** moved to downfield of C-11 (δ_C 209.5 s) and upfield of C-12 (δ_H 2.19; δ_C 49.6 d) in **2**, which suggest a keto-enol tautomerization of C-11 and C-12 in **1** and **2** incurred by the ketalization between C-4 hydroxyl and C-12 keto groups. The

[a]*Key Laboratory of Chemical Biology (Ministry of Education), School of Pharmaceutical Sciences, Shandong University, No. 44 West Wenhua Road, Jinan, Shandong 250012, P. R. China. E-mail: yshen@sdu.edu.cn; Tel: +86-531-88382108*

[b]*State Key Laboratory of Microbial Technology, Shandong University, Jinan, Shandong 250100, P. R. China*

† Electronic supplementary information (ESI) available: Spectroscopic data and other relevant information for compounds **1–6**. CCDC 1481243. For ESI and crystallographic data in CIF or other electronic format see DOI: 10.1039/c7ra06339c

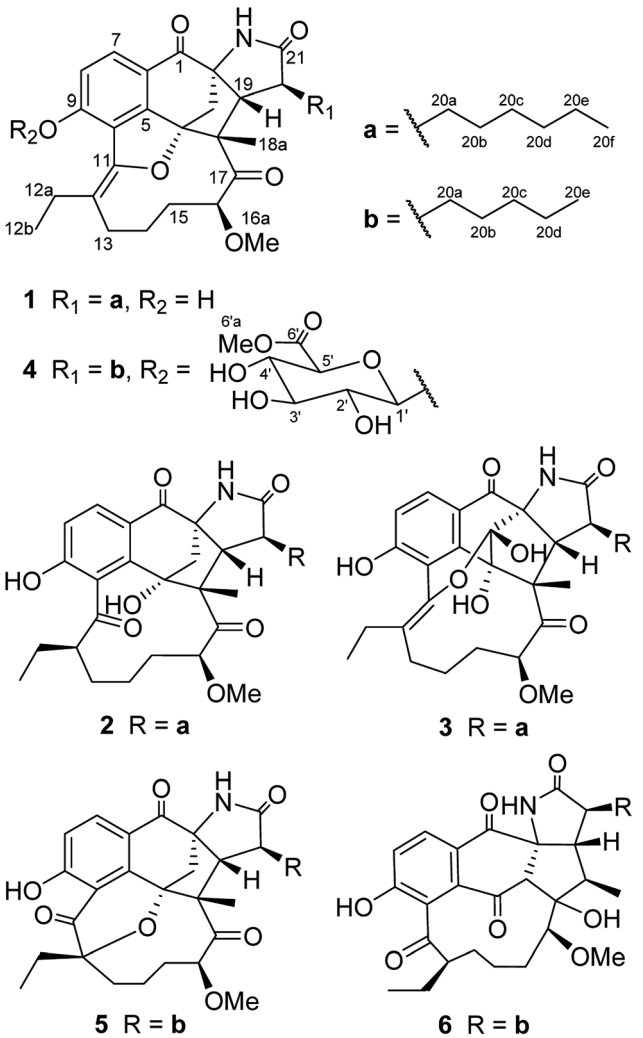

Fig. 1 Structures of compounds 1–6.

molecular weight of **2** was more 18 D than that of **1**, which further demonstrated the hydrolytic cleavage of the ether bond between C-4 and C-11 in **2**. The relative configurations of **2** at C-12, C-16 and C-20 were assigned to be identical to that of 5,10-*seco*-neoansamycin H[14] on the basis of the same biosynthetic origin. Likewise, the relative configurations of **2** at C-18 and C-19 were assigned identical to those of neoansamycin D (**1**) and B[13] on the basis of the same biosynthetic origin.

Neoansamycin F (**3**) with a quasi-molecular ion at *m*/*z* of 554.2748 $[M + H]^+$ was determined to have the molecular formula $C_{31}H_{39}NO_8$. The ^1H and ^{13}C NMR spectra revealed 31 signals, corresponding to four CH_3, nine CH_2, six CH and twelve quaternary C-atoms. The HSQC, ^1H–^1H COSY and HMBC correlations (ESI Table S3 and Fig. S3†) revealed that the structure of **3** was similar to that of **1**. After careful comparison, we found apparent differences including the chemical shifts at C-3 [(δ_C 91.2 s) in **3** and (δ_H 2.46 d, 2.72 d, δ_C 49.9 t) in **1**], which demonstrated the location of hydroxyl at C-3 in **3** instead of methylene in **1**. The NOESY correlations (ESI Table S3†) from H-18a to H-19 and H-20a revealed the relative configurations at C-18, C-19 and C-20 of compound **3**. Considering the identical biosynthetic origin, rest of the configurations of **3** were suggested to be identical to those of neoansamycin D (**1**).

Neoansamycin G (**4**) was determined to have molecular formula $C_{37}H_{47}NO_{12}$ on the basis of HRESIMS (*m*/*z* 698.3172 $[M + H]^+$) (ESI Fig. S32†). The ^1H and ^{13}C NMR data with the aid of HSQC, ^1H–^1H COSY and HMBC experiments revealed that **4** was partially identical to neoansamycin B.[15] The presence of a β-glucuronic acid moiety was revealed by the ^1H NMR signals at δ_H 5.42 (d, J = 7.6 Hz), 3.63 (m), 3.55 (m), 3.67 (m) and 4.18 (d, J = 9.6 Hz) (Table 1), and the ^{13}C NMR signals at δ_C 101.0 d, 74.3 d, 77.8 d, 72.7 d, 76.9 d and 170.7 s (Table 2). These assignments were further confirmed by ^1H–^1H COSY and HMBC correlations. The HMBC correlation from H-6′a (δ 3.77, s, 3H) to C-6′ revealed the presence of 6-*O*-methyl β-glucuronic acid, which was located at C-9 based on the HMBC correlation from the anomeric proton H-1′ to C-9. Thus, the structure of **4** was established to be neoansamycin B-9-*O*-β-glucuronide 6′-methyl ester. The relative configurations of **4** were determined identical to those of **1** on the basis of the same biosynthetic origin.

Neoansamycin H (**5**) was determined as an analogue of **1** with the molecular formula $C_{30}H_{37}NO_7$ (HRESIMS *m*/*z* 524.2642 $[M + H]^+$) (ESI Fig. S39†). The 1D, 2D NMR data (ESI Table S5 and Fig. S5†) revealed that **5** was similarly identical to neoansamycin B.[15] The chemical shifts of C-11 (δ_C 203.8 s) and C-12 (δ_C 85.8 s) in **5** and C-11 (δ_C 148.6 s) and C-12 (δ_C 116.0 s) in neoansamycin B suggested the tautomerization of enol-form and keto-form at C-11 and C-12 in neoansamycin B and **5**, and the downfield shift of C-12 in **5** demonstrated the oxygenation of C-12 and the formation position of the ether bond in **5** is C-4–O–C-12 instead of C-4–O–C-11. The NOESY correlations (ESI Table S5†) from H-12a to H-18a, H-18a to H-19, and H-20a to H-19 revealed the relative configurations of compound **5** at C-12, C-18, C-19 and C-20. The relative configuration of **5** at C-16 was assigned to be identical to that of 5,10-*seco*-neoansamycin H[14] on the basis of the same biosynthetic origin.

The molecular formula of neoansamycin I (**6**) was determined to be $C_{30}H_{39}NO_7$ on the basis of HRESIMS (*m*/*z* 526.2798 $[M + H]^+$). The planer structure was deduced by analysis of its HMQC, ^1H–^1H COSY and HMBC correlations (ESI Table S6 and Fig. S6†). The presence of dihydronaphthoquinone ring and the formation of a five membered ring (C-2/3/17/18/19) were confirmed by the changes of chemical shifts of C-3 (δ_C 70.2 d; δ_H 3.11 s), C-4 (δ_C 195.1 s), C-17 (δ_C 88.8 s) and C-18 (δ_C 40.6 d; δ_H 2.16 m) in **6** and C-3 (δ_C 48.6 t; δ_H 2.31 d & 2.72–2.69 m), C-4 (δ_C 88.6 s), C-17 (δ_C 213.5 s) and C-18 (δ_C 59.9 s) in neoansamycin B.[15] The keto-form of C-11 was deduced on the basis of the chemical shift of C-11 (δ_C 207.9 s) in **6**. The relative configurations of **6** were assigned to be identical to those of neoansamycin D (**1**) on the basis of the same biosynthetic origin.

The antimicrobial activities of **1–6** were measured against *Bacillus subtilis* 86315, *Staphylococcus aureus* ATCC 25923, *Mycobacterium smegmatis* mc^2 155, and *Candida albicans* 5314 by the paper disc diffusion assay (20 μg per disc). Only compounds **1**, **5** and **6** exhibited modest activity against *B. subtilis* 86315 (diameters of inhibitory zones 13, 11, and 9 mm, respectively). In addition, **2** exhibited weak activity against *Staphylococcus aureus* ATCC

Table 1 ^{1}H NMR spectroscopic data for **1–6** (recorded at 600 MHz, δ in ppm, J in Hz; **1**, **2**, **4**, **5** were dissolved in CD_3OD and **3**, **6** in DMSO-d_6)

Pos.	1	2	3	4	5	6
3	2.46, d (9.4) 2.72, d (10.9)	2.29, d (9.6) 3.05, d (10.8)		2.46, d (10.9) 2.76, d (10.9)	2.83, d (10.2) 3.10, d (11.7)	3.11, s
7	7.75, d (8.4)	7.86, d (8.4)	7.64, d (8.4)	7.89, d (8.6)	8.29, d (8.6)	7.85, d (8.6)
8	6.96, d (8.4)	6.96, d (8.4)	7.01, d (8.2)	7.33, d (8.7)	7.15, d (8.7)	7.22, d (8.6)
12		2.21, t (6.9)				2.35, m
13	2.12, m 2.91, m	2.01, m	2.00, m 2.80, m	2.16, m	1.49, m	1.51, m 1.78, m
14	1.68, m	1.62, m	1.59, m 1.80, m	2.01, m	1.83, m 2.00, m	1.45, m
15	1.98, m 1.43, m 2.04, m	1.95, m	1.19, m 1.93, t (13.9)	1.47, m	2.05, m	1.21, m
16	5.02, d (6.0)	4.26, br s	4.81, d (8.0)	5.00, d (7.4)	4.79, d (9.0)	3.24, d (8.3)
18						2.16, m
19	2.25, d (9.8)	2.27, d (8.4)	2.04, d (9.6)	2.28, d (10.0)	2.10, m	2.33, m
20	2.66, m	2.75, m	2.64, m	2.68, m	2.82, m	2.68, m
12a	2.49, m 2.86, m	2.52, m	2.48, m 2.75, m	2.61, m	1.76, m 1.94, m	1.46, m 2.00, m
12b	1.12, t (7.3)	0.93, t (7.8)	1.06, t (7.3)	2.72, m 1.19, t (7.4)	0.80, t (7.3)	0.89, t (7.4)
16a	3.37, s	3.37, s	3.11, s	3.38, s	3.39, s	3.40, s
18a	1.08, s	1.41, s	0.95, s	1.09, s	0.96, s	0.92, d (6.8)
20a	1.91, m	1.70, m	1.19, m 1.72, m	1.89, m	1.53, m	1.49, m
20b	1.55, m	1.27, m	1.19, m 1.51, m	1.29, m	1.27, m	1.19, m 1.26, m
20c	1.32, m	1.45, m	1.23, m	1.37, m	1.24, m	1.22, m
20d	1.29, m	1.29, m	1.22, m	1.32, m	1.30, m	1.25, m 1.28, m
20e	1.33, m	1.30, m	1.28, m	0.92, t (7.1)	0.89, t (6.7)	0.86, t (7.2)
20f	0.91, t (6.7)	0.91, t (6.0)	0.86, t (7.1)			
N–H			8.63, s			7.41, s
1′				5.42, d (7.6)		
2′				3.63, m		
3′				3.55, m		
4′				3.67, m		
5′				4.18, d (9.6)		
6′						
6′a				3.77, s		

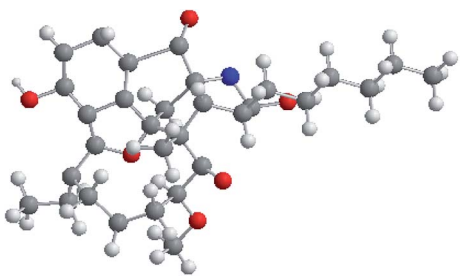

Fig. 2 Single-crystal X-ray structure for neoansamycin D (**1**).

25923 with inhibitory zone of 10 mm. These activities are similar to those of neoansamycins A–C.[15]

Ansamycins are type I polyketide macrolactams.[17] Their highly diversified structures mostly resulted from diverse post-PKS modifications.[12,18] In particular, post-PKS modifications are critical in determining their bioactivities.[3,19] The structures of neoansamycins D–I mirror diverse and interesting post-PKS modifications. However, their antimicrobial activities are moderate unlike other ansamycins usually are potent, implying that broad screening assays are required for exploiting the bioactivities of this class of novel ansamycins.

Experimental

General experimental procedures

Optical rotations were carried out using an Anton Paar MCP200 automatic polarrimeter. The UV spectra were obtained on a TU-1810 spectrophotometer (Beijing Purkinje General Instrument Co., LTD). NMR spectra were recorded on Bruker DRX-600 NMR spectrometer (Bruker Daltonics Inc., Billerica, MA, USA) with tetramethylsilane (TMS) as an internal standard. HRESIMS were carried out on an LTQ-Orbitrap XL. *Sephadex* LH-20 was obtained from GE Amersham Biosciences (25–100 μm; Piscataway,

Table 2 ^{13}C NMR spectroscopic data for compounds **1–6** (recorded at 150 MHz, compounds **1**, **2**, **4**, **5** in CD_3OD and **3**, **6** in DMSO-d_6)

Pos.	1	2	3	4	5	6
1	194.2, C	195.3, C	190.3, C	194.4, C	194.2, C	195.3, C
2	70.0, C	70.1, C	73.9, C	70.2, C	69.7, C	71.2, C
3	49.9, CH_2	51.3, CH_2	91.2, C	50.1, CH_2	52.2, CH_2	70.2, CH
4	89.9, C	95.2, C	94.9, C	90.1, C	84.6, C	195.1, C
5	157.1, C	156.9, C	153.0, C	156.71, C	150.7, C	134.5, C
6	119.0, C	119.2, C	116.3, C	121.4, C	121.3, C	129.3, C
7	129.3, CH	131.8, CH	128.2, CH	129.6, CH	138.0, CH	129.9, CH
8	119.3, CH	119.0, CH	109.0, CH	117.2, CH	119.9, CH	122.4, CH
9	159.1, C	161.4, C	158.7, C	156.72, C	166.7, C	160.8, C
10	118.6, C	121.6, C	117.9, C	121.8, C	114.3, C	124.5, C
11	150.3, C	209.5, C	149.5, C	149.8, C	203.8, C	207.9, C
12	118.7, C	49.6, CH	115.7, C	120.9, C	85.8, C	53.5, CH
13	30.0, CH_2	29.8, CH_2	28.4, CH_2	30.5, CH_2	26.5, CH_2	29.6, CH_2
14	25.14, CH_2	26.0, CH_2	24.5, CH_2	25.1, CH_2	19.8, CH_2	25.4, CH_2
15	32.4, CH_2	30.0, CH_2	30.4, CH_2	32.4, CH_2	35.1, CH_2	30.5, CH_2
16	88.7, CH	92.5, CH	85.4, CH	88.7, CH	87.1, CH	82.6, CH
17	215.9, C	214.2, C	211.1, C	215.9, C	214.8, C	88.8, C
18	61.9, C	60.1, C	57.7, C	61.9, C	63.0, C	40.6, CH
19	60.6, CH	61.2, CH	56.5, CH	60.7, CH	61.1, CH	56.6, CH
20	46.8, CH	45.6, CH	44.6, CH	46.9, CH	45.9, CH	42.3, CH
21	180.4, C	180.7, C	178.7, C	180.4, C	180.2, C	178.2, C
12a	25.08, CH_2	24.6, CH_2	23.3, CH_2	25.6, CH_2	35.0, CH_2	27.1, CH_2
12b	15.3, CH_3	13.2, CH_3	14.9, CH_3	15.0, CH_3	8.6, CH_3	11.3, CH_3
16a	58.8, CH_3	58.4, CH_3	56.7, CH_3	58.9, CH_3	57.5, CH_3	61.9, CH_3
18a	31.2, CH_3	25.4, CH_3	31.1, CH_3	31.2, CH_3	27.5, CH_3	10.2, CH_3
20a	31.8, CH_2	31.5, CH_2	30.9, CH_2	31.9, CH_2	31.2, CH_2	32.6, CH_2
20b	27.2, CH_2	26.8, CH_2	25.3, CH_2	27.0, CH_2	26.6, CH_2	24.4, CH_2
20c	30.7, CH_2	23.5, CH_2	29.1, CH_2	33.4, CH_2	33.2, CH_2	31.4, CH_2
20d	23.7, CH_2	33.3, CH_2	31.7, CH_2	23.7, CH_2	23.6, CH_2	22.0, CH_2
20e	32.9, CH_2	23.6, CH_2	22.1, CH_2	14.4, CH_3	14.5, CH_3	14.0, CH_3
20f	14.4, CH_3	14.4, CH_3	14.0, CH_3			
1′				101.0, CH		
2′				74.3, CH		
3′				77.8, CH		
4′				72.7, CH		
5′				76.9, CH		
6′				170.7, C		
6′a				53.0, CH_3		

New Jersey) and LiChroprep RP-18 were used for column chromatography (CC) from Merck (40–63 μm; Darmstadt, Germany). Semi-preparative HPLC were performed on an Agilent 1200 equipped with a ZORBAX Eclipse XDC_{18} 5 μm column (9.4 × 250 mm).

Fermentation and eextraction

The mutant strain SR201*nam1*OE was cultured on ISP3 medium (oatmeal 30 g, saline salt 1 mL, agar 20 g, pH 7.2) for 14 days at 28 °C. The culture (a total volume of 100 liters) was chopped, diced and extracted three times overnight with an equal volume of EtOAc/MeOH 80 : 20 (v/v) at room temperature and partitioned between ddH_2O and EtOAc until the EtOAc layer was colorless. Then, the EtOAc extract was dried with Na_2SO_4, and the solvent was removed under vacuum at 38 °C. The EtOAc extract was partitioned with petroleum ether (PE) and MeOH until the PE layer was colorless. The MeOH solution was concentrated under vacuum at 38 °C to obtain MeOH extract (40 g).

Isolation and ppurification of compounds 1–7

The MeOH extract (40 g) was subjected to column chromatography over Sephadex LH-20 (120 g) eluted with MeOH to obtain 5 fractions (Fr. 1–5). Fr. 3 (11 g) was chromatographed over Sephadex LH-20 (120 g) eluted with MeOH to obtain 3 fractions, Fr. 3a–3c. Fr. 3b (6.7 g) was subjected to MPLC over RP-18 silica gel (80 g), and 20 subfractions with 200 mL for each gradient were obtained from the elution with 30, 50, 60, 70, 75, 80 and 100% MeOH, respectively. In accordance with TLC results, 4 fractions, Fr. 3b1–3b4 were obtained. Fr. 3b2 (3.1 g) was subjected to CC over Sephadex LH-20 (120 g) eluted with MeOH to obtain 4 fractions, Fr. 3b2a–3b2d. Fr. 3b2c (984 mg) was further subjected to MPLC over RP-18 silica gel (80 g) eluted with 30%, 40%, 50%, 55%, 60% and 100% CH_3CN to obtain Fr. 3b2c1–3b2c4. Fr. 3b2c2 (105.2 mg) were purified by semi-preparative HPLC (eluted with 50% acetonitrile, 4 mL min^{-1}, UV 320 nm) to yield **4** (3 mg). Fr. 3b2c3 (213 mg) were purified by semi-preparative HPLC (eluted with 55% acetonitrile in 0.05% formic acid, 4 mL min^{-1}, UV 320 nm) to yield **3** (1.7 mg), and **6** (1.2 mg).

Fr. 3b3 (2.93 g) was subjected to CC over Sephadex LH-20 (120 g) eluted with MeOH to obtain 3 fractions, Fr. 3b3a–3b3c. Fr. 3b3b (1.03 g) was further subjected to MPLC over RP-18 silica gel (80 g) eluted with 30%, 40%, 50%, 55%, 60%, 70% and 100% CH_3CN to obtained Fr. 3b3b1–3b3b4. Fr. 3b3b3 (153 mg) were purified by semi-preparative HPLC (eluted with 65% acetonitrile in 0.05% formic acid, 4 mL min^{-1}, UV 320 nm) to yield **7** (6.0 mg), **1** (3.0 mg), **2** (2.3 mg) and **5** (8.2 mg).

Compound 1. Light yellow crystal; $[\alpha]_D^{20} = -15.80$ (*c* 0.100, MeOH); UV (MeOH) λ_{max} (log ε): 306 (2.23), 275 (2.55) nm; ^1H and ^{13}C NMR data, see Tables 1 and 2; HRESIMS: *m*/*z* 522.2848 $[M + H]^+$ (calcd for $C_{31}H_{40}NO_6^+$, 522.2850).

Compound 2. Yellow powder; $[\alpha]_D^{20} = -20.52$ (*c* 0.077, MeOH); UV λ_{max} (log ε): 303 (2.28), 277 (2.58) nm; ^1H and ^{13}C NMR data, see Tables 1 and 2; HRESIMS: *m*/*z* 540.2952 $[M + H]^+$ (calcd for $C_{31}H_{42}NO_7^+$, 540.2956).

Compound 3. Light yellow powder; $[\alpha]_D^{20} = -32.10$ (*c* 0.057, MeOH); UV (MeOH) λ_{max} (log ε): 306 (2.25), 277 (2.58) nm; ^1H and ^{13}C NMR data, see Tables 1 and 2; HRESIMS: *m*/*z* 554.2748 $[M + H]^+$ (calcd for $C_{31}H_{40}NO_8^+$, 554.2748).

Compound 4. Yellow powder; $[\alpha]_D^{20} = -24.70$ (*c* 0.100, MeOH); UV (MeOH) λ_{max} (log ε) 311 (2.16), 280 (2.50) nm; ^1H and ^{13}C NMR data, see Tables 1 and 2; HRESIMS: *m*/*z* 698.3172 $[M + H]^+$ (calcd for $C_{37}H_{48}NO_{12}^+$, 698.3170).

Compound 5. Red powder; $[\alpha]_D^{20} = -84.22$ (*c* 0.270, MeOH); UV (MeOH) λ_{max} (log ε) 304 (2.07), 275 (2.38) nm; ^1H and ^{13}C NMR data, see Tables 1 and 2; HRESIMS: *m*/*z* 524.2642 $[M + H]^+$ (calcd for $C_{30}H_{38}NO_7^+$, 524.2643).

Compound 6. Light yellow powder; $[\alpha]_D^{20} = -46.25$ (*c* 0.040, MeOH); UV (MeOH): λ_{max} (log ε) 302 (2.10), 270 (2.43) nm; ^1H and ^{13}C NMR data, see Tables 1 and 2; HRESIMS: $C_{30}H_{39}NO_7$, *m*/*z* 526.2798 $[M + H]^+$ (calcd for $C_{30}H_{40}NO_7^+$, 526.2799).

X-ray crystallographic analysis

The single-crystal X-ray diffraction intensity data of **1** were collected with a Bruker SMART-1000 diffractometer using graphite-monochromated Mo Kα radiation ($\lambda = 0.71073$ Å) by the ω-scan technique [scan width 0–180°, $2\theta \leq 50°$] at 293 (2) K.

Crystal data of neoansamycin D (**1**): $C_{31}H_{39}NO_6$, $M_r = 521.67$, orthorhombic, $a = 8.5601$ (9) Å, $b = 14.9864$ (13) Å, $c = 23.2722$ (18) Å, $\alpha = 90°$, $\beta = 90°$, $\gamma = 90°$, $V = 2985.5$ (5) $Å^3$, space group *P*2 (1) 2 (1) 2 (1), $Z = 4$, Dx = 1.232 mg m^{-3}, μ (Mo Kα) = 0.698 mm^{-1}, and $F(000) = 1192$. Crystal dimensions: 0.32 × 0.28 × 0.27 mm^3. Independent reflections: 4528 ($R_{int} = 0.0495$). Theta range for data collection: 3.51 to 66.19°. The final $R_1 = 0.0778$, $wR_2 = 0.1356$ ($I > 2\sigma(I)$). CCDC number: 1481243.†

Antimicrobial assay

The antimicrobial activities of compounds **1–6** against *Candida albicans* 5314, *Staphylococcus aureus* ATCC 25923, *Mycobacterium smegmatis* mc^2 155, *Pseudomonas aeruginosa* PA01, *Bactllus subtilis* 86315 or *Salmonella enterica* serovar Typhimurium UK-1 χ8956 were measured with a paper disc diffusion assay.[20] Kanamycin and amphotericin were used as positive control.

Conclusions

In summary, we isolated and characterized six neoansamycin congers, namely neoansamycins D–I (**1–6**), with unusual extender units and diverse post-PKS modifications from the *Streptomyces* sp. SR201*nam1*OE strain. In particular, although various unusual extender units have been found in other polyketide-derived structures,[21] this study is the first example that *n*-hexylmalonyl-CoA was used in the biosynthesis of ansamycins. The promiscuity of neoansamycin PKS could facilitate the bioengineering of novel ansamycins.[11,22]

Acknowledgements

This work was supported in part by the National Natural Science Foundation of China (81373304, 81530091, U1405223), and the Independent Innovation Foundation of Shandong University (IIFSDU, 2014JC027) and Program for Changjiang Scholars and Innovative Research Team in University (IRT_17R68).

Notes and references

1 H. G. Floss and T. W. Yu, *Chem. Rev.*, 2005, **105**, 621–632.
2 L. Whitesell, E. G. Mimnaugh, B. De Costa, C. E. Myers and L. M. Neckers, *Proc. Natl. Acad. Sci. U. S. A.*, 1994, **91**, 8324–8328.
3 J. M. Cassady, K. K. Chan, H. G. Floss and E. Leistner, *Chem. Pharm. Bull.*, 2004, **52**, 1–26.
4 H. X. Wang, Y. Y. Chen, L. Ge, T. T. Fang, J. Meng, Z. Liu, X. Y. Fang, S. Ni, C. Lin, Y. Y. Wu, M. L. Wang, N. N. Shi, H. G. He, K. Hong and Y. M. Shen, *J. Appl. Microbiol.*, 2013, **115**, 77–85.
5 C. Lu, Y. Li, J. Deng, S. Li, Y. Shen, H. Wang and Y. Shen, *J. Nat. Prod.*, 2013, **76**, 2175–2179.
6 S. Li, C. Lu, J. Ou, J. Deng and Y. Shen, *RSC Adv.*, 2015, **5**, 83843–83846.
7 S. Li, H. Wang, Y. Li, J. Deng, C. Lu, Y. Shen and Y. Shen, *ChemBioChem*, 2014, **15**, 94–102.
8 G. Zhao, S. Li, Z. Guo, M. Sun and C. Lu, *RSC Adv.*, 2015, **5**, 98209–98214.
9 S. R. Li, G. S. Zhao, M. W. Sun, H. G. He, H. X. Wang, Y. Y. Li, C. H. Lu and Y. M. Shen, *Gene*, 2014, **544**, 93–99.
10 J. Zhang, Z. Qian, X. Wu, Y. Ding, J. Li, C. Lu and Y. Shen, *Org. Lett.*, 2014, **16**, 2752–2755.
11 G. Shi, N. Shi, Y. Li, W. Chen, J. Deng, C. Liu, J. Zhu, H. Wang and Y. Shen, *ACS Chem. Biol.*, 2016, **11**, 876–881.
12 X. Li, J. Zhu, G. Shi, M. Sun, Z. Guo, H. Wang, C. Lu and Y. Shen, *RSC Adv.*, 2016, **6**, 88571–88579.
13 Z. Zhang, X. Wu, R. Song, J. Zhang, H. Wang, J. Zhu, C. Lu and Y. Shen, *RSC Adv.*, 2017, **7**, 14857–14867.
14 Z. Zhang, J. Zhang, R. Song, Z. Guo, H. Wang, J. Zhu, C. Lu and Y. Shen, *RSC Adv.*, 2017, **7**, 5684–5693.
15 S. Li, Y. Li, C. Lu, J. Zhang, J. Zhu, H. Wang and Y. Shen, *Org. Lett.*, 2015, **17**, 3706–3709.
16 J. Zhang, S. Li, X. Wu, Z. Guo, C. Lu and Y. Shen, *Org. Lett.*, 2017, **19**, 2442–2445.
17 H. G. Floss, *J. Nat. Prod.*, 2006, **69**, 158–169.

18 X. Wang, Y. Zhang, L. V. Ponomareva, Q. Qiu, R. Woodcock, S. I. Elshahawi, X. Chen, Z. Zhou, B. E. Hatcher, J. C. Hower, C.-G. Zhan, S. Parkin, M. K. Kharel, S. R. Voss, K. A. Shaaban and J. S. Thorson, *Angew. Chem., Int. Ed.*, 2017, **56**, 2994–2998.
19 P. Spiteller, L. Bai, G. Shang, B. J. Carroll, T. W. Yu and H. G. Floss, *J. Am. Chem. Soc.*, 2003, **125**, 14236–14237.
20 D. Raahave, *Antimicrob. Agents Chemother.*, 1974, **6**, 603–605.
21 N. Quade, L. Huo, S. Rachid, D. W. Heinz and R. Müller, *Nat. Chem. Biol.*, 2012, **8**, 117–124.
22 Y. Tian, N. Jiang, A. H. Zhang, C. J. Chen, X. Z. Deng, W. J. Zhang and R. X. Tan, *Org. Lett.*, 2015, **17**, 1457–1460.